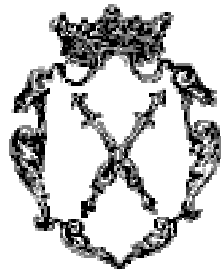


Marian Smoluchowski Institute of Physics  
Jagiellonian University



Particle Track Identification in the Drift Chambers  
of the BRAHMS Experiment

Radosław Karabowicz  
Master thesis  
Advisor: prof. dr hab. Zbigniew Majka

# Contents

<b>1. Introduction</b>	
1.1 Motivation for building RHIC .....	2
1.1.1 Short introduction to the physics of URHIC .....	2
1.1.2 What is RHIC? .....	3
1.1.3 Experiments at RHIC .....	3
1.2 BRAHMS experiment .....	4
1.2.1 Description of the spectrometers at BRAHMS .....	4
1.2.2 The Drift Chambers .....	7
<b>2. Software</b>	
2.1 BRAT .....	11
2.1.1 What is BRAT? .....	11
2.2 Organization of the tracking software .....	11
2.2.1 DC Software .....	11
2.2.2 Global software .....	13
<b>3. Tracking</b>	
3.1 Local tracking .....	13
3.2 Drift chambers tracking improvement .....	14
3.2.1 Performance of the drift chambers .....	14
3.2.2 New tracking procedure .....	15
3.2.3 Realization of the new tracking procedure .....	15
3.2.3a Detectors used .....	15
3.2.3b Step-by-step description of the method .....	16
<b>4. Efficiency</b>	
4.1 Justification of the efficiency optimization .....	21
4.2 Methods of the efficiency calculation .....	22
<b>5. Results</b>	
5.1 Track resolution in the drift chambers .....	26
5.2 Efficiency of the drift chambers .....	26
<b>6. Conclusions</b>	
6.1 Usefulness of the introduced software in the BRAHMS experiment .....	27
6.2 Possible extensions to the whole FS –farther development .....	27
<b>A. The BRAHMS Collaboration</b> .....	29
<b>B. The BRAT Classes (Selected)</b> .....	30

# 1. Introduction

## 1.1 Motivation for RHIC facility construction

### 1.1.1 Short introduction to the physics of URHIC

UltraRelativistic Heavy Ion Collisions (URHIC) became recently a very rapidly developing part of the physics. Combining nuclear physics and elementary particle physics it is a unique and innovative field of experimental researches. Modern era of the experiments with high-energy heavy ions took place in the 1986 in the Brookhaven National Laboratory (BNL) at the Alternate Gradient Synchrotron (AGS) where various ions up to  $^{28}\text{Si}$  were accelerated to 14.5 GeV per nucleon (AGeV). Soon after beams of relativistic heavy ions were accessible at the Super Proton Synchrotron (SPS) in the European Center for Nuclear Research (CERN). SPS accelerated  $^{16}\text{O}$  at 60 and 200 AGeV in 1986, and in the next year  $^{32}\text{S}$  at 200 AGeV.

To accelerate really heavy ions the world of physicists had to wait until 1992, when first experiments with  $^{197}\text{Au}$  at 11.4 AGeV took place at the AGS. Completely new regime was achieved in 1995 at the SPS, where beams of  $^{208}\text{Pb}$  were accelerated to 158 AGeV.

The next barrier was overcome in the year 2000 and following by the Relativistic Heavy Ion Collider (RHIC) at the BNL, where beams of  $^{197}\text{Au}$  are accelerated in opposite directions up to 100 AGeV. The first collisions at RHIC were carried out at slightly lower energy, i.e.  $\sqrt{s} = 130\text{AGeV}$  in the center-of-mass frame (which in this case coincides with the laboratory frame), and the maximum energy, that is  $\sqrt{s} = 200\text{AGeV}$ , was reached in year 2001.

Ultrarelativistic collisions of heavy ions are characterized by very large particle multiplicities, i.e. in a collision a great number of particles are produced. It has already been seen in Au-Au collisions at AGS and in Pb-Pb collision at SPS, where total charged particles multiplicity exceeded 450 and 1500, respectively. The multiplicities at the energies accessible at RHIC are still higher reaching (for 5% most central collisions)  $3860 \pm 300$  [1] at  $\sqrt{s} = 130\text{AGeV}$  and  $4630 \pm 370$  [2] at  $\sqrt{s} = 200\text{AGeV}$ .

The other exciting field of interest is measuring the antiparticles to particles ratios. At RHIC the following values were found at  $y=0$ :  $0.75 \pm 0.05$ ,  $0.95 \pm 0.03$  and  $1.01 \pm 0.03$  for  $\text{pbar}/\text{p}$ ,  $\text{K}^-/\text{K}^+$  and  $\pi^-/\pi^+$ , respectively.

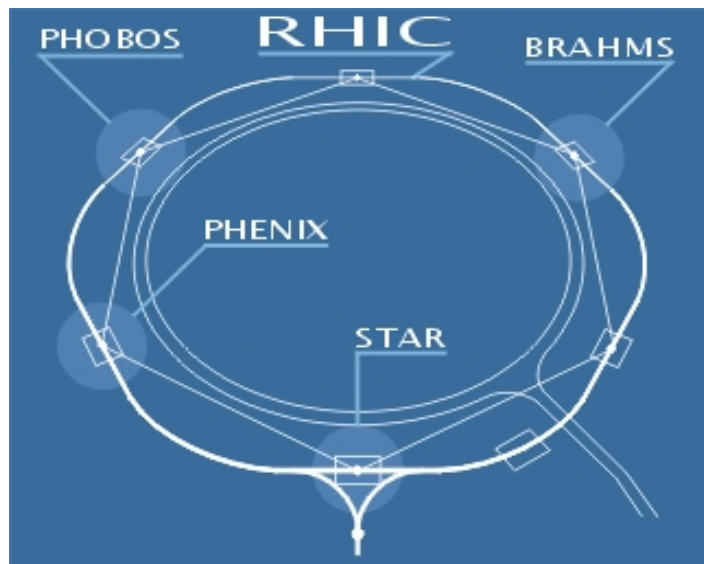
At the lower energies (i.e. about 1 AGeV) the multiplicities and the  $\text{pbar}/\text{p}$  ratios are much smaller and the exact studies shown that the colliding nuclei are stopped, the density and temperature increase. At the AGS and SPS energies the temperatures are still higher, but on the contrary the matter is not fully stopped but rather a certain degree of transparency is obtained. Also the baryon chemical potential decreases. The collisions at yet higher energies currently available at RHIC should be characterized by even higher transparency, net baryon density close to zero, and very high temperature. These are the conditions in which

Quantum ChromoDynamics (QCD) predicts phase transition of the strongly interacting nuclear matter to a new state called Quark-Gluon Plasma (QGP). The calculations for zero net baryon density place the critical temperature at about 160 MeV.

### 1.1.2 What is RHIC?

Relativistic Heavy Ion Collider (RHIC) is currently the largest and most powerful accelerator. The facility is located in the Brookhaven National Laboratory (BNL) and started its operation in the year 2000. The main design was to accelerate gold nuclei to energy 100 GeV per nucleon but other nuclei and protons will also be used. The facility is the collider so the energy of the crashing gold nuclei is 200 AGeV per pair of nucleons, which in head-on gold-gold collision gives 39.4 TeV.

Fig. 1. Almost 1.5 km in diameter RHIC ring and position of the experiments: BRAHMS (sharing place with pp2pp), STAR, PHENIX and PHOBOS.



### 1.1.3 Experiments at RHIC

RHIC facility was constructed with purpose to give place to 6 experiments. Nowadays on RHIC there are located 5 experiments named STAR, PHENIX, PHOBOS, BRAHMS and pp2pp. The exact location of them is shown in the Fig. 1. STAR and PHENIX are the biggest experiments that base on the barrel detectors. Main goal of the PHOBOS is to analyze low transverse momentum properties of the collisions. BRAHMS advantage over other experiments is the greatest range in the rapidity, that is:  $|y| < 4$ . The pp2pp experiment is dedicated to the proton-proton collisions.

## 1.2 BRAHMS experiment

BRAHMS collaboration consists of about 60 physicists from 12 institutions in 6 countries. The list of the collaboration is given in the Appendix A. One of the biggest groups in the BRAHMS is the group from the Marian Smoluchowski Institute of Physics of the Jagiellonian University, where three of the BRAHMS' detectors were built, namely the Drift Chambers.

### 1.2.1 Description of the spectrometers at BRAHMS

BRAHMS detector setup consists of various detectors, which can be roughly assembled into 5 groups (see Fig. 2).

The first group is the multiplicity detectors. There are two: Tiles Multiplicity Array (TMA) and Silicon Multiplicity Array (SiMA) arranged into hexagonal barrels around the nominal collision point – Interaction Region (IR). Their main task is to measure the multiplicity of the event. This information is used among other things for triggering, but the main target aimed at is the determination of the centrality of the collision: the bigger the multiplicity the more central collision. Figure 3 presents multiplicity for  $\sqrt{s} = 130 A GeV$ .

## BRAHMS Experimental Setup

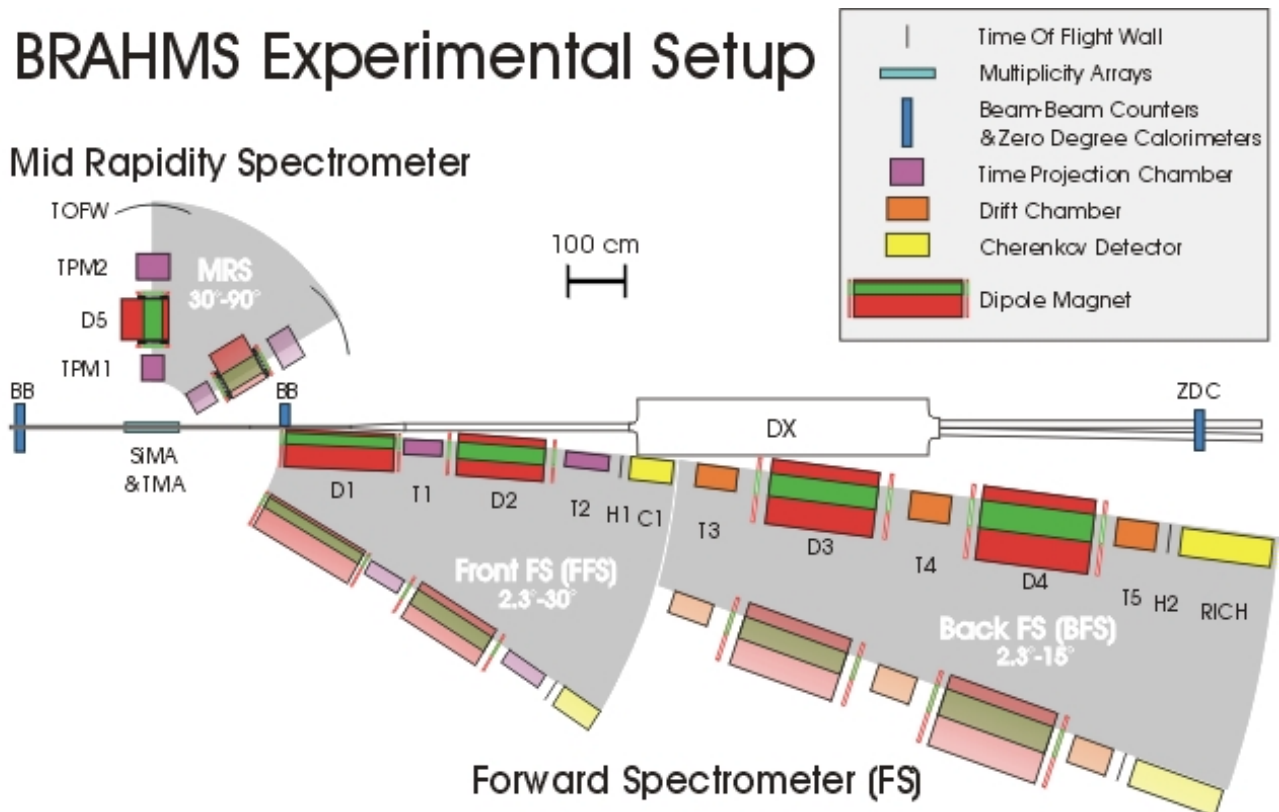


Fig. 2. BRAHMS experimental setup. Gray fields show the ranges of the spectrometers, the solid and transparent shapes represent various detectors and magnets in their extreme positions.

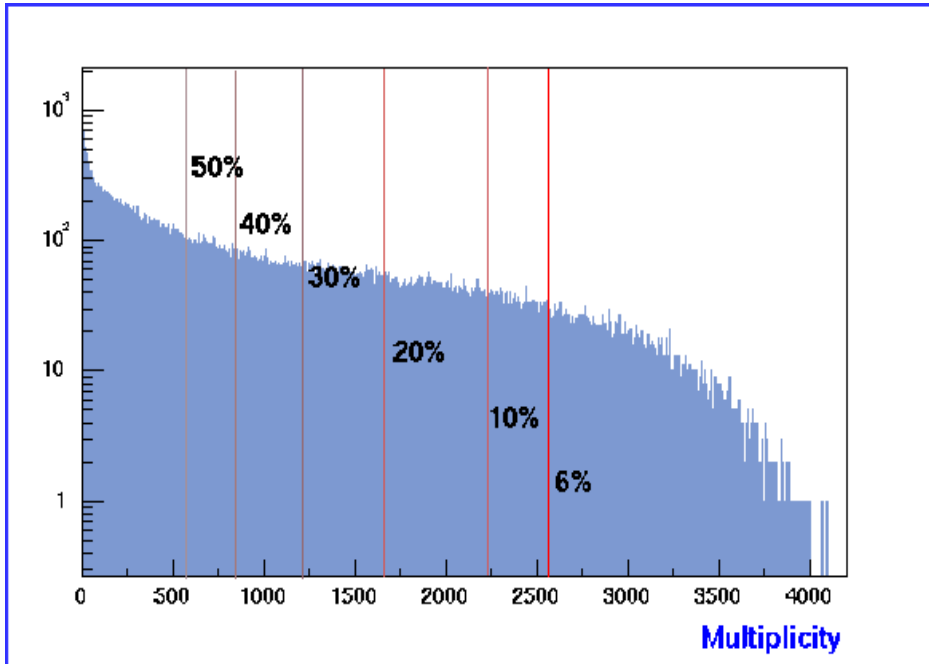


Fig 3. Sum of the SiMA and TMA multiplicity distribution for AuAu collisions at  $\sqrt{s} = 130 AGeV$ .

Zero Degree Calorimeter (ZDC) and Beam-Beam Counters (BB) constitute the second group of the detectors, which can be called the detectors of the vertex. They are the basic trigger in the event, but they also determine the vertex position along beam axis with accuracy to 0.65 cm and the timing to about 50 ps. Figure 4 presents combination of results from these detectors. The collision in the IR is roughly equally distant from both BB detectors and from both ZDCs. This means that the time difference ( $\Delta t$ ) in the arrival of the signals should be close to 0 for both BB and ZDC. These collisions are responsible for the central peak in Fig. 4, which shows the very first collisions observed on June the 15<sup>th</sup>, 2000, in the BRAHMS experiment. The two side peaks are created in the processes that occur outside the IR, e.g. during the collisions of the projectiles with the impurities in the beam-pipe.

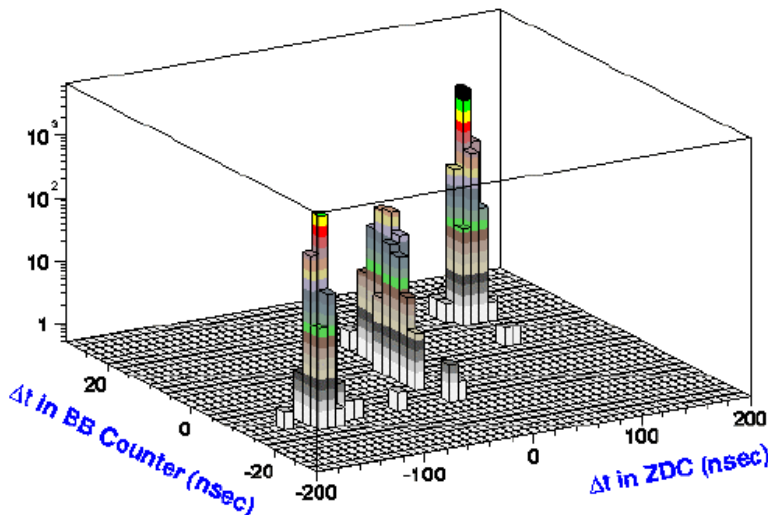
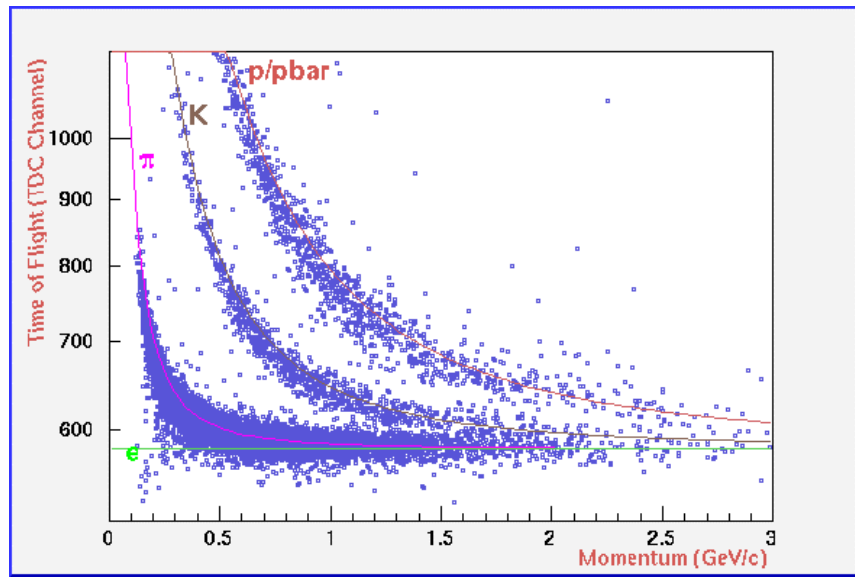


Fig. 4. First collisions observed in the BRAHMS experiment.

The third group is the Mid Rapidity Spectrometer (MRS), which consists of two Time Projection Chambers (TPM1 and TPM2) placed on both sides of the dipole magnet (D5). TPM1 faces the IR directly. Time Of Flight Wall (TOFW) is placed right after TPM2 and is used for time-of-flight measurements. Momentum is determined from tracking in the time projection chambers and matching the tracks via D5 magnet. Momentum and time-of-flight measurements lets the particle identification in a considerably large dynamical range, namely  $\pi/K$  up to 2.2 GeV/c, and K/p up to 3.7 GeV/c (see Fig. 5).

Fig. 5. The Time-Of-Flight vs. Momentum plot for the MRS at  $90^\circ$ . The solid curves show theoretical predictions.



Furthermore, the tracking in the TPM1 allows yet more precise determination of the vertex position, both in beam and vertical directions. MRS is movable from  $90^\circ$  to  $30^\circ$  in respect to the beam direction, thus covering wide range in rapidity round 0, that is  $-0.1 < y < 1.3$ .

The remaining groups, Front (FFS) and Back (BFS) Forward Spectrometers are very similar in concept to the MRS, and are combined in to the Forward Spectrometer (FS). FFS can be moved from  $2.3^\circ$  to  $30^\circ$  (thus covering almost 3 units in rapidity, i.e.  $1.3 < y < 4$ ), and BFS moves from  $2.3^\circ$  to  $15^\circ$ , in respect to the beam. FFS consists of two Time Projection Chambers (T1 and T2) separated by dipole magnet (D2) and preceded by another magnet (D1). T2 is further succeeded by the Time Of Flight wall (TOF1) and Cherenkov Detector (C1). It alone can identify  $\pi/K$  up to 3.3 GeV/c, and K/p up to 5.7 GeV/c. In the high rapidity region it is supported by the BFS, consisting of three Drift Chambers (DC) named T3, T4 and T5, separated by two dipole magnets (D3 and D4). Behind T5 another time of flight wall (TOF2) and Ring Imaging Cherenkov (RICH) are placed thus expanding the overall acceptance up to 30 GeV/c (without RICH:  $\pi/K$  up to 5.0 GeV/c, and K/p up to 8.5 GeV/c). FFS and BFS are placed on different platforms, hence are totally independent, though it is most useful when aligned in line.

### 1.2.2 The Drift Chambers

The concept of the BRAHMS experiment was made up before year 1996, and so was the conceptual design of all the detectors and the set-up. According to BRAHMS Conceptual Design Report [3] T3, T4 and T5 detectors were to be the drift chambers, with active area of about  $40 \times 30 \text{ cm}^2$  for T3 and  $50 \times 35 \text{ cm}^2$  for T4 and T5. The required track resolution was to be about  $300 \mu\text{m}$ .

They were built [4] in the Hot Matter Physics Division at the Marian Smoluchowski Institute of Physics of the Jagiellonian University and placed on the spectrometer platform in 1999.

The basic unit of the drift chamber is the detection cell rectangular in shape. The center of the cell is occupied by the anode wire ( $\phi=20 \mu\text{m}$ , gold-plated tungsten), while on its sides there are cathode wires ( $\phi=80 \mu\text{m}$ , beryllium-copper). This configuration of wires together with the so called field wires generate and shape the electric field inside the cell. Furthermore the anode wires are detecting the ionization electrons created for example by a particle passing through the cell. The set of such parallel drift cells form a plane, called a detection plane. Single detection plane does not provide us with the exact point through which a particle passed, but rather a distance of the line parallel to the sense wire, specified by the time of electron drift generated away from it. This fact suggests that the drift chamber should consist of at least two planes, each having wires arranged in different directions, called views. Only a very short consideration discloses the main inconvenience, that is in the case of the  $N=2$  tracks in the detector there would be  $N^2=4$  crossings and thus it would be really hard to find a track. This fact requires introduction of another plane, which would have wires arranged in yet another direction. It is not unusual to have even more views, which only improve the track recognition. Therefore in the drift chambers at the BRAHMS experiment there are 4 views, named X, Y, U and V. In the X view wires are placed vertically (and thus supplies information about the horizontal position of the track, in Y – horizontally (but information is vertical). The wires in the U and V views are bend by  $+18^\circ$  and  $-18^\circ$  in respect to the wires in the X view. Such a set-up is the direct consequence of the simple fact that the magnet sweep particles in the horizontal direction and thus to obtain the best momentum resolution the horizontal position of the track must be reconstructed with incredible accuracy.

The other inconvenience connected with the drift chambers is that we know which wire gave a signal and the distance between the track and the anode wire, but still we do not know the side on which the particle passed the wire. This problem, called the left-right ambiguity, can be solved by using two planes in every view with another condition that the drift cells in the subsequent plane is staggered. The distance of the stagger in the DCs at BRAHMS is  $\frac{1}{4}$  of the drift cell as shown in Fig. 6.

Each DC consists of 3 modules with 10 (for T3) or 8 (T4, T5) detection planes arranged into four different views (the details are given in the Table 1). Figures 7 present an example of an event with two tracks in the drift chamber.



Table 1. Basic information about the drift chambers at the BRAHMS experiment. Description is given in the text.

Detector	Number of modules	Planes	View type	View angle [deg]	Number of sense wires	Sense wire spacing [cm]	Stagger distance [cm]
T3	3	1,2,3	x,x,x	0	40	1,1,1	0.0,0.25,0.0
		4,5	y,y,y	90	30	1,1,1	0.0,0.25,0.0
		6,7,8	u,u	18	48	1,1	0.0,0.25
		9,10	v,v	-18	48	1,1	0.0,0.25
T4	3	1,2	x,x	0	23	2.2,2.2	0.0,1.1
		3,4	y,y	90	16	2.2,2.2	0.0,1.1
		5,6	u,u	18	27	2.2,2.2	0.0,1.1
		7,8	v,v	-18	27	2.2,2.2	0.0,1.1
T5	3	1,2	x,x	0	23	2.2,2.2	0.0,1.1
		3,4	y,y	90	16	2.2,2.2	0.0,1.1
		5,6	u,u	18	27	2.2,2.2	0.0,1.1
		7,8	v,v	-18	27	2.2,2.2	0.0,1.1

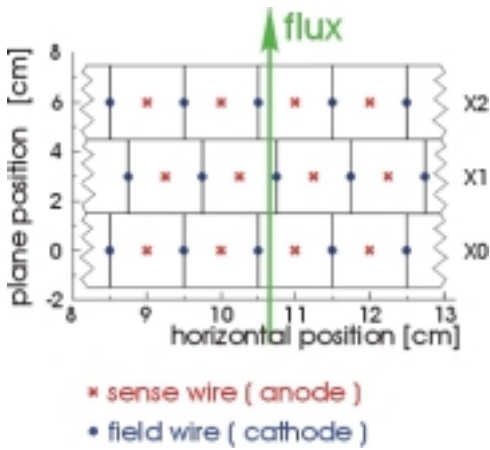


Fig. 6. Scheme of the wires layout in the X planes of the T3.

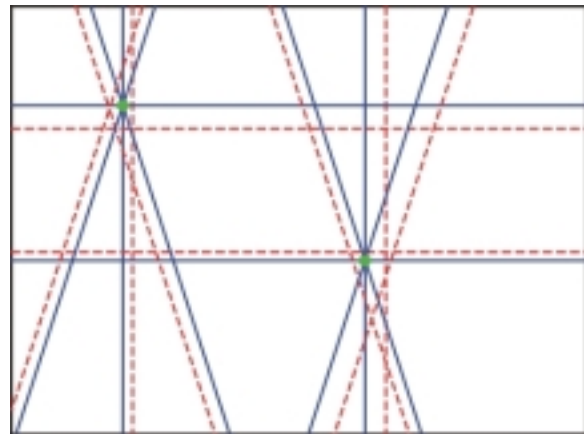


Fig. 7a). Projection of hits in a two-tracks event (drift chamber with 4 planes only). The red, dashed lines show the false hits resulting from the left-right ambiguity.

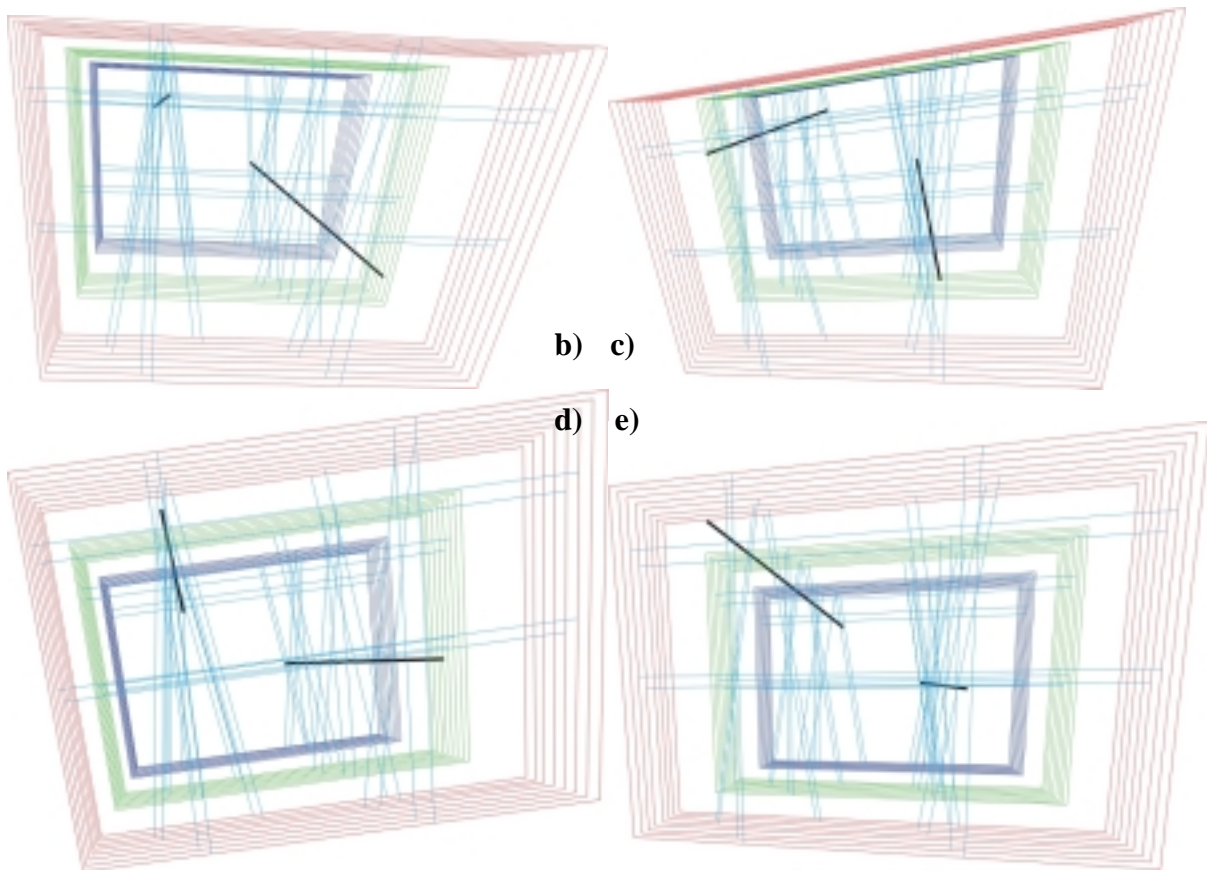


Fig. 7b)c)d)e). Example of an event with two tracks in the drift chambers (T5), the wires that detected the ‘particle’ are shown.

A charged particle passing through the detection cell travels in the gas that fills the drift chamber ( $66\%Ar+33\%C_4H_{10}+1\%$ ethylene vapor)<sup>1</sup>. Along the particle track free electrons are created in well-known process – the ionization. The electrons move in the strong electric field towards the anode wire. The arrival of the electrons provides the start for the measurement, while specially delayed signal from the triggering systems provides the stop. The time difference between the two signals, converted to the digit by the TDC, is proportional to the drift distance, but shifted (among others by the value of the trigger delay) and reversed (i.e. the signals with smaller TDC values come from the tracks more distant from the sense wire). Figure 8 presents the TDC spectrum from the T3 detector. The first step of the calibration is to find the position of the slope on the right side of the plot, which can be different for each wire and for each run. Figure 9 presents reversed and shifted TDC spectrum, which now can be treated as the drift time of the ionization electrons. The drift time equal to zero clearly corresponds to the drift distance equal to zero. The next problem is to find the drift time that corresponds to the maximum drift distance, equal to 0.5 cm in case of the T3 (see Table 1). Figure 10 presents integrated drift time spectrum. The time of  $145\mu s$

<sup>1</sup> The gas mixture was chosen from among few others ( $66\%Ar+33\%C_4H_{10}$ ,  $75\%Ar+25\%C_4H_{10}$ ,  $85\%Ar+15\%C_4H_{10}$ , all with small admixture of vapour ethylene). The chosen composition gave the highest efficiency and the best track resolution

corresponding to the distance of 0.5cm was chosen arbitrarily<sup>2</sup>. The drift distance is calculated assuming the linear dependence between the drift time and drift distance. The result of the calibration is shown in the Figure 11. For detailed description see [4].

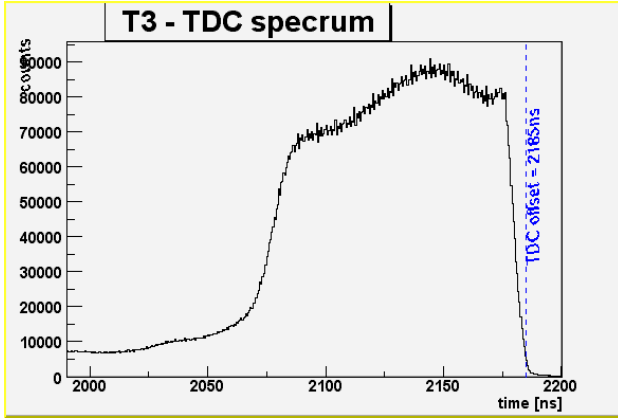


Fig. 8. TDC spectrum from T3 (for all wires).

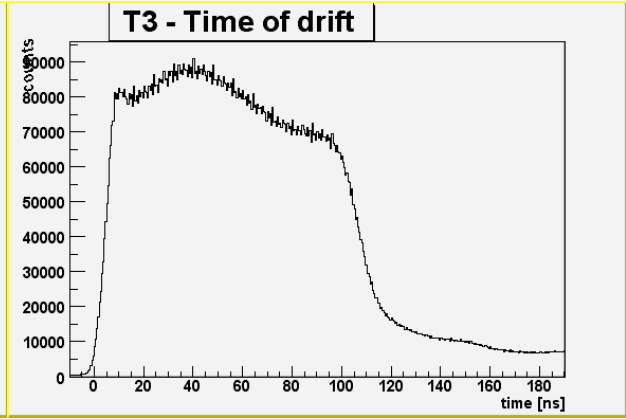


Fig. 9. Reversed and shifted TDC spectrum.

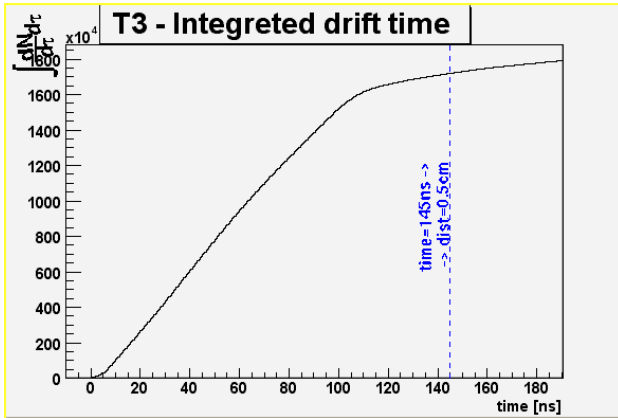


Fig. 10. Integrated TDC spectrum (in reverse direction). Time of drift equal to 145ns corresponds to the drift distance of 0.5 cm.

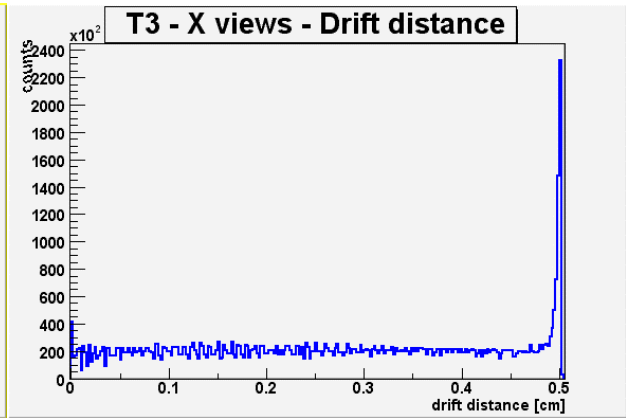


Fig. 11. Drift distance for hits on all wires in the X view.

The good performance of the detectors is generally suppressed by the large background (particular troublesome in the case of the gold-gold collisions at the RHIC energies, with multiplicities exceeding 4000 particles in one event) and the multi-particle events, when there is a need of reconstructing several track inside the detector. But these disadvantages are surely compensated by exquisitely good track resolution, of about 130 $\mu$ m, and reaching even 90 $\mu$ m.

<sup>2</sup> Different values of the maximum drift time were studied and the track resolution was compared. The chosen value (145 $\mu$ m) gave the best track resolution.

## 2. Software

### 2.1 BRAT

#### 2.1.1 What is BRAT?

The BRAHMS experimental hardware, which in every event gathers about 10K parameters, needs complicated and specialized software. The core of this software is called the BRahms Analysis Tool (BRAT). The best description of it is presented in the [5]. The software is compatible with the ROOT [6], which is a powerful tool for the data processing, created by the physicists from the CERN. The language of the programming is the CINT, which bases on the C++. The basic ideas of the programming language (called the Object Oriented Programming – OOP) are the classes, which in BRAT can be divided (owing to the class functionality) in to:

- data classes,
- modules,
- managers,
- utilities.

The data classes, as the name indicated, contain data of different types, from the raw data through calibration and geometry information to the Rdo (Reduced data objects – i.e. calibrated raw data) and containers, which are the collections of any data. The modules do most of the analysis since they manipulate the data. Some are responsible for combining raw data with calibration and geometry files and creating the Rdo data – these are called the Rdo modules, others fit the particle trajectories to the data – the tracking modules, and so on. The managers manage the data used by different modules to ensure that various modules use the same data, which may be particularly important in case of different geometry of calibration files (which may happen in the early stages of the program development when this kind of files are rather frequently updated). The last and smallest group are the utilities, which generally incorporates the classes that does not belong to any of the above groups –e.g. the mathematical functions, vectors, lines, planes, etc.

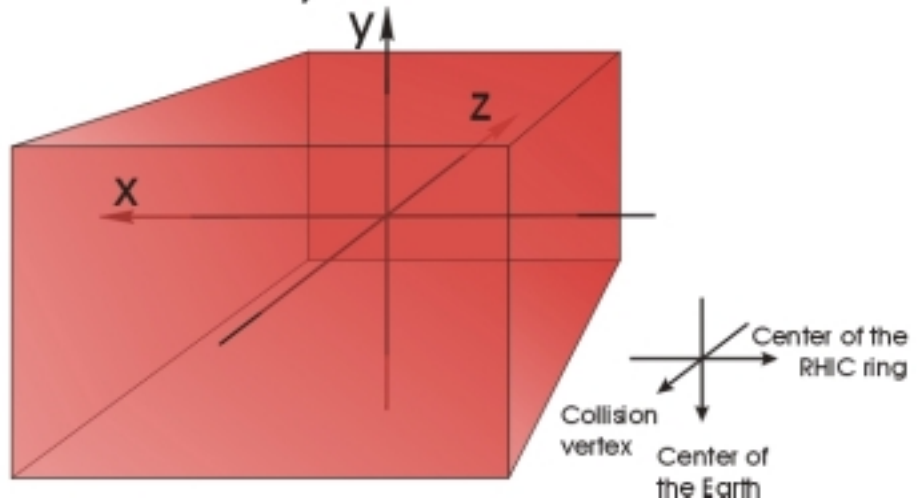
### 2.2 Organization of the tracking software

#### 2.2.1 DC Software

The local drift chamber coordinate system, shown in Fig. 12, is as follows: the origin is in the geometrical center of the detector, the  $x$  axis is horizontal, parallel to all detection planes, the  $y$  axis is vertical pointing up, and the  $z$  axis is horizontal, perpendicular to the detection planes, and equivalent to the direction of movement of the collision products.

## Coordinate system in the drift chambers

Fig. 12. Local coordinate system in the drift chambers.



The drift chambers' software follows the ordinary way (Fig.13) of the other detectors. The raw data is recorded in a digitized form, which is readable as the data table (`BrDataTable3`) of the objects belonging to the class called `BrDcDig`.

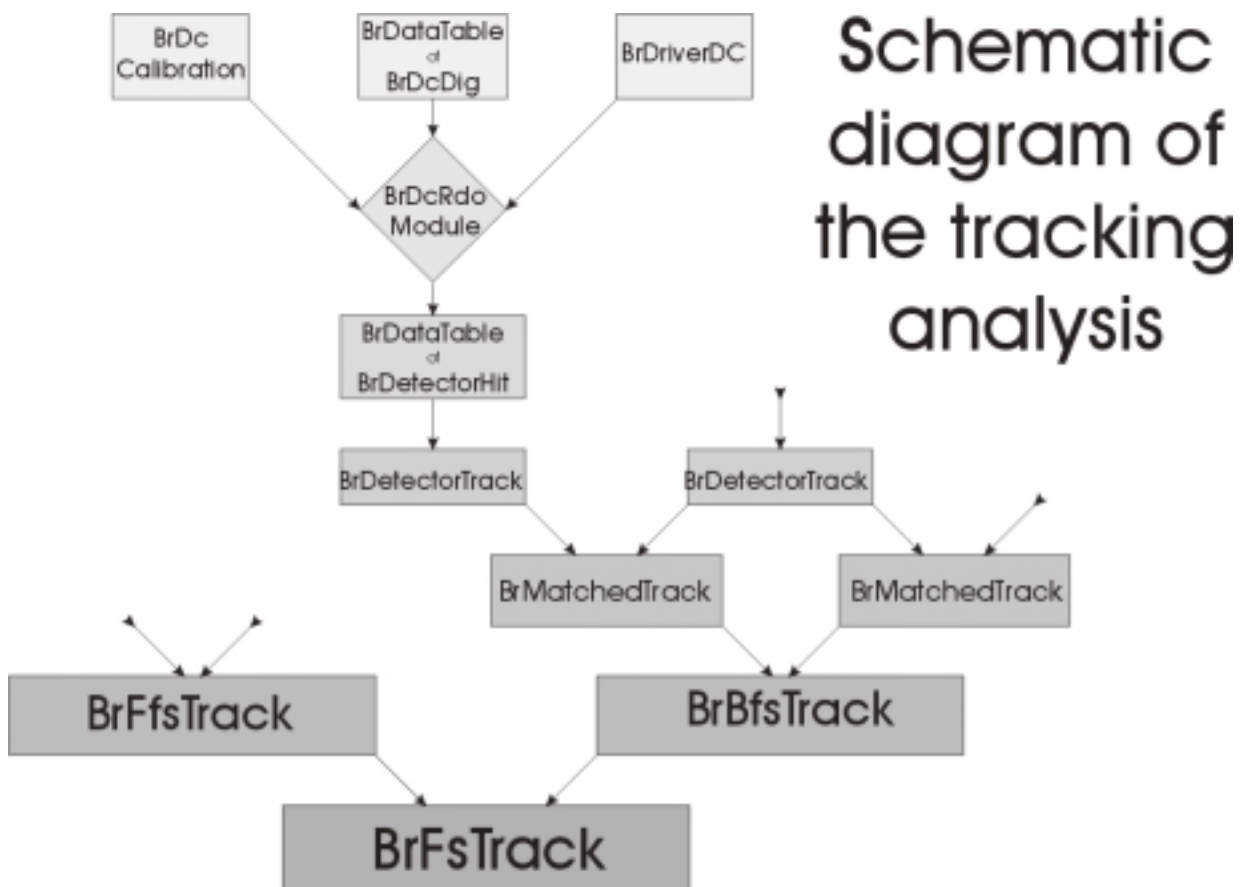


Fig. 13. Organization of the tracking software for the drift chambers in the BRAHMS experiment.

<sup>3</sup> The more detailed description of the classes mentioned in this section is given in appendix B.

The information stored in the BrDcDig cannot be used directly in the tracking analysis – it has to be combined with the calibration and geometrical data. The module responsible for creating the reduced data objects for the drift chambers is called BrDcRdoModule, and was introduced to BRAT on April the 11<sup>th</sup>, 2002 by author of this thesis. The additional information that is needed to create the Rdo data is acquired from the database via special classes, BrDriverDC (geometry) and BrDcCalibration (the calibration process is described in section 1.2.2).

It is not necessary to know the number of the module and of the plane, but the  $z$  position of the plane and the symbol of the view (i.e. X, Y, U or V). Furthermore, the number of the wire should be transformed to the distance from the middle of the given plane, while the TDC signal should be converted to the drift distance. While the first transformation is the result of a survey then the latter information bases on the calibration files. The BrDcRdoModule creates a new BrDataTable of the reduced data objects (see App. B).

This module greatly simplifies the tracking in the drift chambers by elimination of the using of the BrDriverDC and BrDcCalibration.

The reduced data are subsequently used in the tracking modules (the tracking method is described in section 3.1) that creates BrDataTable of BrDetectorTracks.

### 2.2.2 Global software

On this level all the problems connected with the local tracking, specific for various kinds of detectors, are overcome. The next problem is connected with the switching from the local to global coordinates, and this is solved by special classes called BrGeometryDbManager and BrParameterDbManager. The class named BrModuleMatchTrack joins any two BrDetectorTracks separated by one magnet in to one object called BrMatchedTrack. They contain pointers to the tracks they were created from, the momentum of the particle reconstructed from tracks entering and exiting the magnet, and the status, which describes the quality of the connection.

The BrMatchedTracks created using the tracks in the drift chambers are further combined by BrBfsTrackingModule into a BrBfsTrack, which together with BrFfsTrack constitutes the BrFsTrack – the final goal of the tracking – which contains all the reconstructed information about the particle, its kind, charge, momentum, mass, time-of-flight and so on.

## 3. Tracking

### 3.1 Local tracking

The tracking in the BRAHMS experiment is divided into few steps, the lowest of which is the local tracking. The main class for containing local tracks is BrDetectorTrack, which holds information about track position, direction and its

unique ID. Construction of the detector track is specific for various kinds of the detectors, i.e. for TPCs and DCs, since methods used in the tracking are diametrically different.

Figure 13 shows various steps of the tracking in the drift chambers on a hypothetical two dimensional drift chamber. The first step to do is to reduce the raw data to the Rdo's, which is done by the BrDcRdoModule – the result can be seen in Fig. 14a – there is detailed information about the position of the hits. The next step in the tracking is the hits clusterization (by BrDCClusterFinder), which combines hits from different planes and views in each module separately. This generally solves two things. First, by combining hits from the same views it deals with the left-right ambiguity – and this is shown on Fig. 14b. Moreover, by combining hits from different views it narrows hits from the initial lines to more-or-less precise points. The clusters themselves do not only include information about the position of the track in a given module, but also contains approximate information about its direction/slopes. This information is then used in the BrDCTrackingModule for final combining of the clusters (compare Fig. 14c) into a BrDetectorTrack.

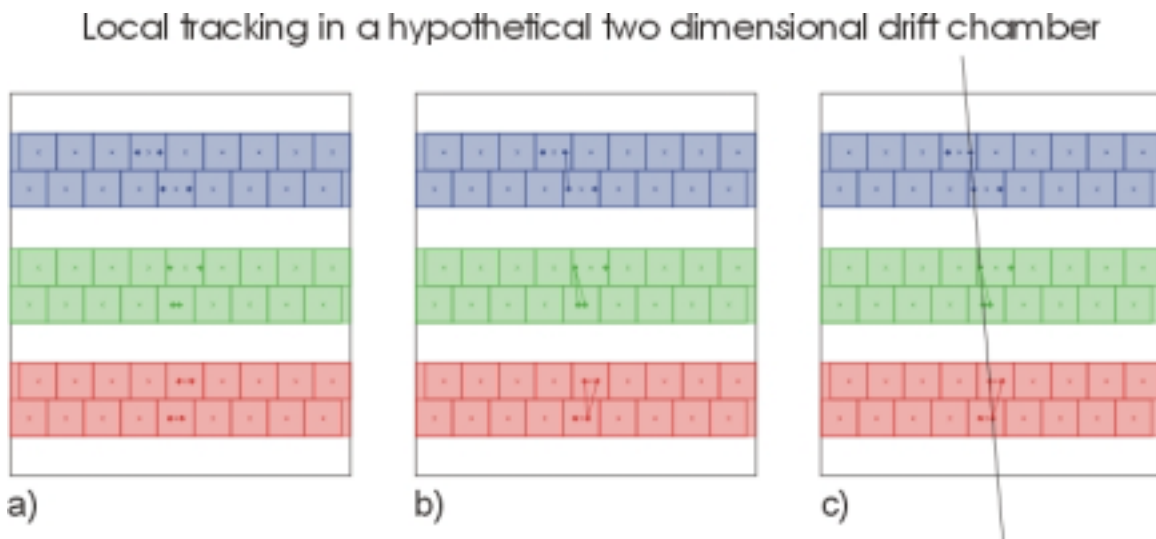


Fig. 14. Various steps of the local tracking in a hypothetical two-dimensional drift chamber – details are given in the text.

## 3.2 Drift chambers tracking improvement

### 3.2.1 Performance of the drift chambers

There are a lot of reasons that can affect efficiency and resolution of the DCs. T3 detector is placed in the position that is directly exposed to secondary particles that originate from the DX magnet (RHIC magnet). The background in the T5 is considerably smaller, and most of it are the particles coming from the RHIC tunnel. By far the best situation is in the case of the T4 detector, which is sheltered by the D3 and D4 magnets. But these are very common conditions for the detectors to work in. The real problem occurs, when something goes wrong. And that was what happened towards the end of the Year 2001 run when the 2<sup>nd</sup>

module of the T5 failed, presumably due to a broken wire. Quick repair was impossible as all of the specialists were in Poland at that time. Therefore it was decided to gather the data with one module of the T5 off, and then to remedy it on the data-analysis stage. And that was the time when the idea of the new tracking method was born.

### 3.2.2 New tracking procedure

As T5 was not fully operating the idea was to use other detectors in the tracking, i.e. to track locally in the neighboring detector and then to project the track-line into the detector and thus try to reconstruct the track using only the hits, which were closest to the line. The first problem to deal with was the fact that T5 is separated from the next tracking detector T4 by the D4 magnet, which enforces that the probe track must be swept through this magnet which in general is not trivial as the tracking in the detector does not provide momentum information, which is on the other hand essential for tracing particle through the magnet.

The solution to the problem is to find the momentum of the particle from another detectors. Combining tracks in the T3 and in the T4 (using BrModuleMatchTrack) into the BrMatchedTracks gives us not only the particle momentum (taken from the D3 magnet) but also the track is confirmed in another detectors, thus increasing the probability that the track should be found in the T5.

### 3.2.3 Realization of the new tracking procedure

#### 3.2.3a Detectors used

The idea of using the T3 and T4 tracks (combined into BrMatchedTrack, which contains information about the track/particle momentum) to tracking in the T5 can be extended. Since the particles travel ‘undisturbed’ by any magnet between T2 and T3 then the T3 tracks can be replaced by the T2 tracks. Hence in the analysis T2-T4 and T3-T4 matched tracks are used. The schematic layout of the detectors used for tracking in the T5 detector is shown on Fig. 15a. Figure 15b presents analogous scheme for tracking in the T3, which, as mentioned before, is very noisy due to the high background. In this case T4-T5 and T2-T4 matched tracks are used. Counting the probe and reconstructed tracks it is possible to determine the efficiency of these two detectors, i.e. T3 and T5. Comparing the result with the hits on the Time-Of-Flight walls (H1 and H2, for T3 and T5, respectively) is a good way of calculating the TOFs efficiency.

Fig. 15a. Detectors used in case of tracking in the T5.





Fig. 15b. Detectors used in case of tracking in the T3.



### 3.2.3b Step-by-step description of the method

Figure 16 shows various steps of the reconstruction method. The first figure from the set presents non-ideal situation in the drift chamber. Two particles passed the hypothetical detector, one of which was a background particle, which nevertheless created hits. There are also shown additional hits, which can sometimes spontaneously arise in the strong electric field as well as a case of single-wire inefficiency and thus lack of hit in the cell traversed by the particle. Tracking in this event would be particularly difficult, and almost impossible in a drift chamber devoid of the middle module.

Dashed line shown in the Fig. 16b presents a projection of the track from a neighboring detector. The most important feature shown here is that the projected track does not necessarily correspond directly with the true particle trajectory. The other thing to observe here is that sometimes the projected track may irrevocably point at some hit, which was not created by the true particle.

The next step towards reconstructing the trajectory in the drift chamber is the choosing of the hits. Two possible methods were taken into consideration when constructing the tracking procedure:

- The first idea was to choose the closest hits to the projected track in every plane. The reasons presented above quickly eliminated the idea by the observation that the hits chosen in this way are not necessarily the best ones nor the ones created by the particle. In the case when the particle would not create hit in a given plane, but still on the very same plane there would be a hit somewhere far away it would not be a good idea to use it for tracking. Furthermore, if the projected track would be closer to the wrong one of a pair of the hits created by the particle due to the left-right ambiguity, it too would be senseless to choose it for further analysis.
- The second idea seems to eliminate these disadvantages and was therefore chosen. In this method a small tube is created around the projected track, and only the hits from inside the tube are used in later analysis. The width of the tube is carefully matched on the basis of the few plots, shown in Fig. 17. These plots presents the difference between the distance of the track to the center of a given plane and the distance of all the hits in this plane to its center, in the T5 detector.

## New tracking method in a hypothetical two dimensional drift chamber

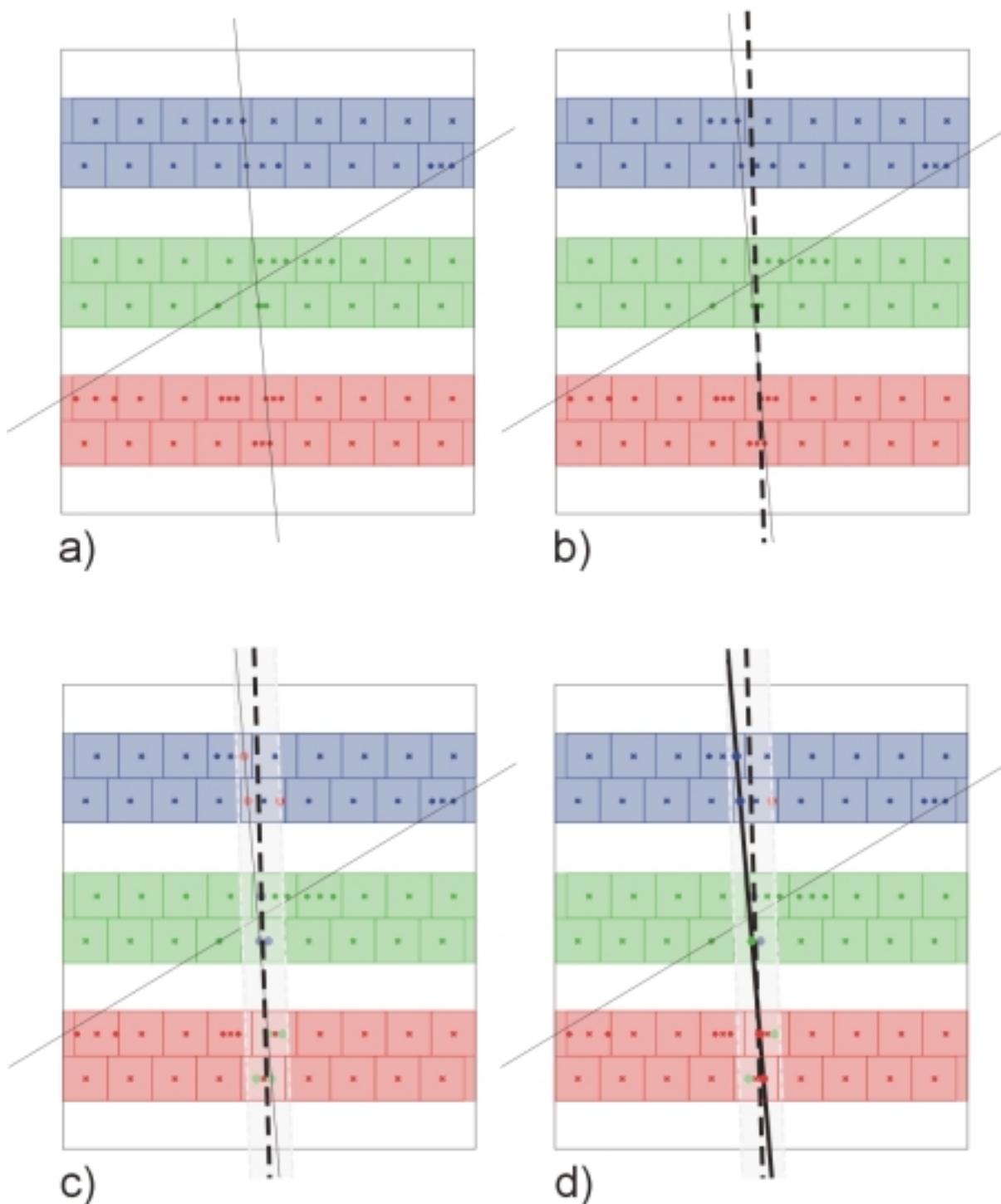


Fig. 16. Consecutive steps of the new tracking method. a) shows hypothetical drift chamber with two particles, one of which does not pass other detectors and was probably some background secondary, the inefficiency of the detector and some ghost hits are also shown. b) – the dashed line shows projected track from other detectors, which *does not* necessarily agrees completely with the real track. c) shows the ‘tube’ around the projected track and accepted hits (in the figure – different color). d) the line shows the fitted trajectory using only hits that fulfilled the given conditions.

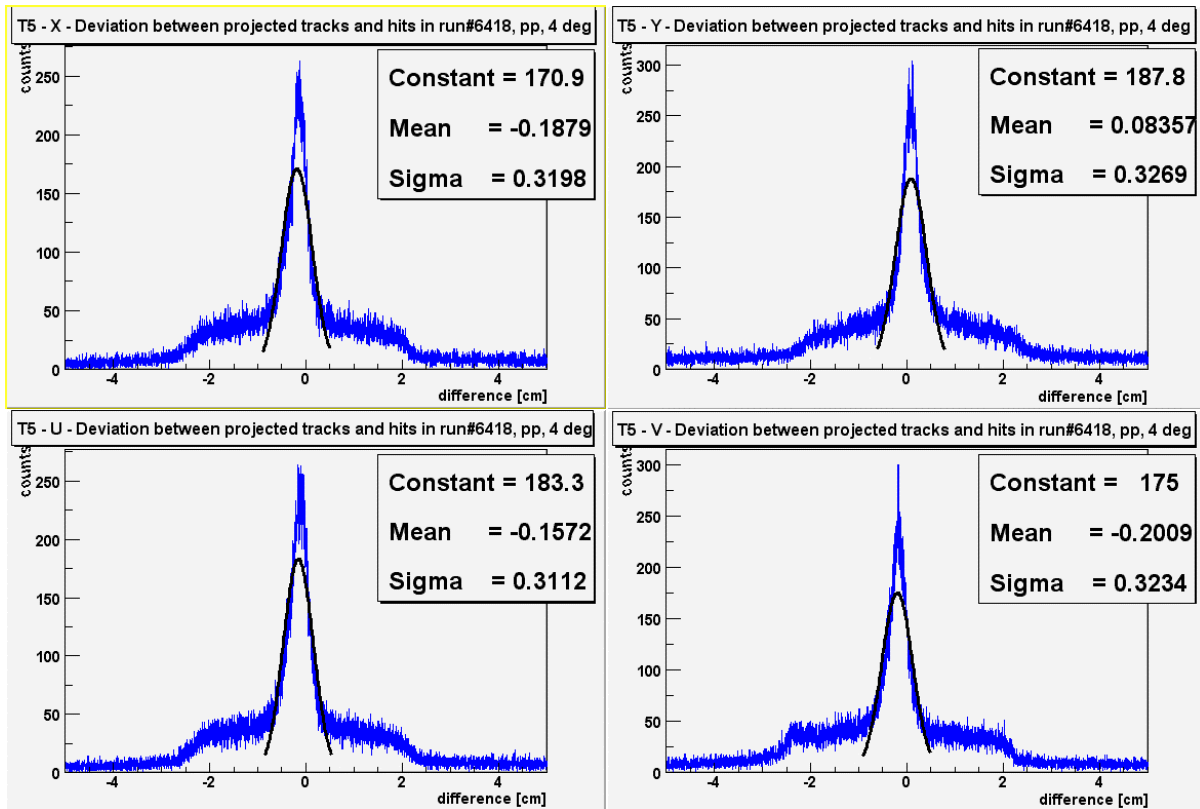


Fig. 17. The distances between the projected track and the hits in the T5 detector, in different views – description is given in the text.

The most important feature of this figure is that the central peak that can be and is interpreted as the hits created by the particle is shifted with respect to the 0, which means that the projection of the track via D4 magnet is *not* perfect, but rather the particles tend constantly to bend more than it would result from the sweeping the particle trajectory using the momentum taken from the D3 magnet. Besides the hits in the middle there is also a considerably wide hill clearly protruding the overall background (which is very small in the T5) and ranging from approximately  $-2.2\text{cm}$  to  $2.2\text{cm}$ . If the width of the cell in the T5 is taken into account (that is  $2.2\text{ cm}$ ) then this is easily explained as the hits resulting from the left-right ambiguity.

Fitting the gaussian curve to the central peak one can calculate average offsets and sigmas that will be used for accepting hits in the further analysis. The tube is then shifted a little bit in respect to the projected track (by the offset) and its width is equal to  $3 \cdot \text{sigma}$ , in order to accept all the hits which constitute the middle peak in the Fig.17. Table 2 shows offsets and sigmas for different setups used on this stage.

Table 2. Offsets and sigmas for creating the tube – see the text.

	T3				T5			
	Au-Au		p-p		Au-Au		p-p	
	offset [ $\mu\text{m}$ ]	sigma [ $\mu\text{m}$ ]	offset [ $\mu\text{m}$ ]	sigma [ $\mu\text{m}$ ]	offset [ $\mu\text{m}$ ]	sigma [ $\mu\text{m}$ ]	offset [ $\mu\text{m}$ ]	sigma [ $\mu\text{m}$ ]
X	0.25	0.37	0.35	0.33	-0.15	0.36	-0.20	0.34
Y	0.06	0.35	0.07	0.29	0.04	0.36	0.04	0.32
U	0.25	0.36	0.35	0.32	-0.13	0.36	-0.17	0.33
V	0.22	0.36	0.31	0.32	0.14	0.36	-0.21	0.33

The next stage of the analysis decides whether one can accept or not the event. Required conditions are:

- number of accepted hits (hits in the tube),
- number of views that had a hit,
- number of accepted hits per view.

Table 3 gives the requirements applied, for different detectors.

Table 3.  
Required conditions for accepting the projected track.

detector \ demanded	T3	T5	T5 (2 <sup>nd</sup> module out of order)
hits	18	16	8
planes	17	15	7
views	3	3	3
planes in the X view	5	4	2
planes in the Y view	5	4	2
planes in the U view	3	3	1
planes in the V view	3	3	1

To every hit accepted for further analysis the ID is set to 0. Hits chosen in this way are the basis to fit a track using a least-square method. As can be seen in Fig. 16, not all the hits which were accepted belong to the real track. This suggests that some kind of cleaning must be applied. The cleaning (described below) is made in steps, during which only one hit is marked (the ID is set to 1). After every step the new track is fitted to all the hits that were not marked, i.e. only to the ones with ID equal to 0.

There are two stages of cleaning. The first one tries to manage the left-right ambiguity. The hits are arranged in an array, position in which depends on the distance to the track. The function marks the first hit from the array if inside the tube was more than one hit from this plane. The second stage marks the hit which distance from the track is the largest, with the condition that it must be larger than 500 $\mu\text{m}$ . This value was arbitrary chosen basing on the track resolution in the drift chambers. As can be seen later on in this section and in the paragraph 6, the track resolution is better than 150 $\mu\text{m}$ , which suggests that 99.7% of the hits belonging

to a track should be within  $450\mu\text{m}$  from the track (as  $450\mu\text{m} = 3 \cdot 150\mu\text{m}$ ). The condition was set to  $500\mu\text{m}$  to ensure that no hits belonging to the track are lost.

After the cleanings the program ends up with a track, with a certain number of associated hits and with some parameters. In order to accept the track, it has to fulfill few conditions – it cannot vary too much from the original probe track and it must be fitted to a sufficient number of hits. The former requirements are taken from the plots showing comparison of parameters of the tracks, that is the differences in the slopes (ax, ay) and in the positions (x0, y0) between the projected and fitted tracks. Figures 18 show the plots, one can see the track conformity, though with certain offsets. To confirm the process of the reconstruction two conditions must be fulfilled – see Table 4. The first condition is that the track must be based on a sufficient number of hits. The second condition combines the number of required hits with the number of parameters not varying too much between the reconstructed and projected track. It means that if all the parameters are within the boundaries (set by sigmas and offsets from Fig. 18) then a smaller number of hits is required than in the case when fewer (2 or 3) parameters are confirmed. Figures 19 present track reconstruction resolutions in different views in the T5 detector.

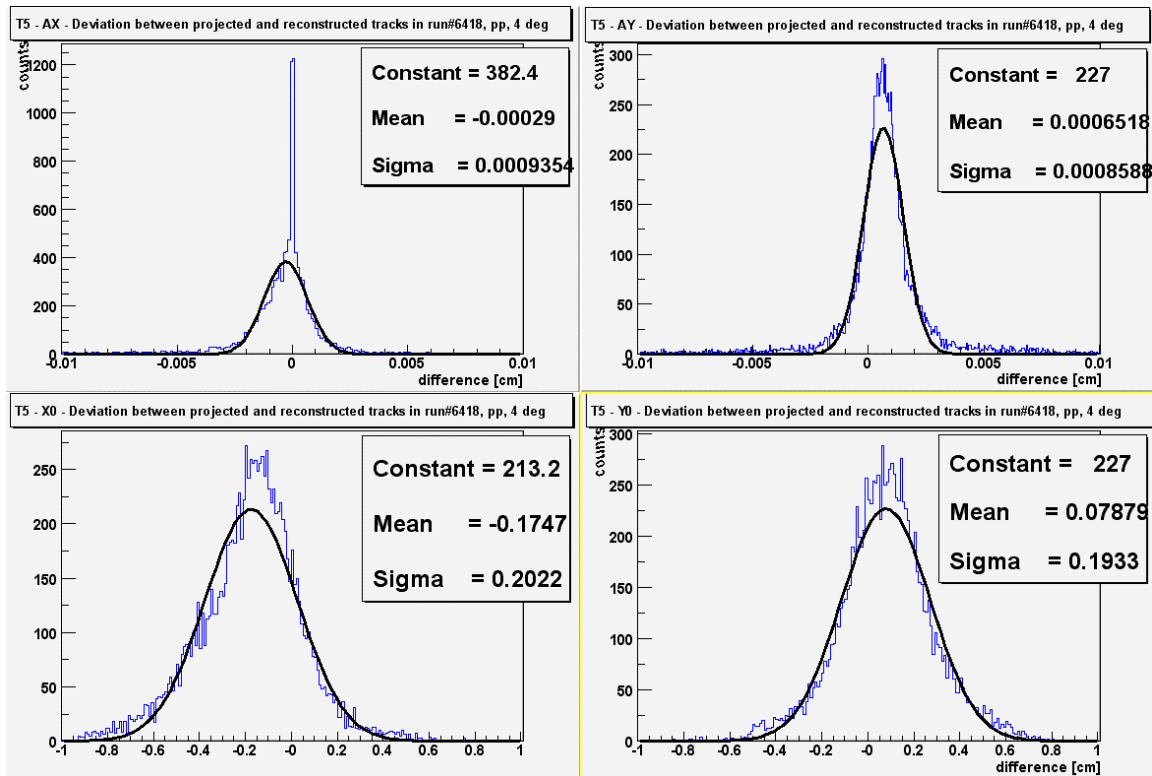


Fig. 18. Comparison of projected and reconstructed tracks in the T5 detector.

Table 4.  
Required conditions for accepting the reconstructed track.

required \ detector	T3	T5	T5 (2 <sup>nd</sup> module out of order)
1 <sup>st</sup> condition: number of required hits	15	11	8
2 <sup>nd</sup> condition: number of confirmed parameters * number of required hits (separately)	57 (4*15) (3*19) (2*29)	44 (4*11) (3*15) (2*22)	32 (4*8) (3*11) (2*16)

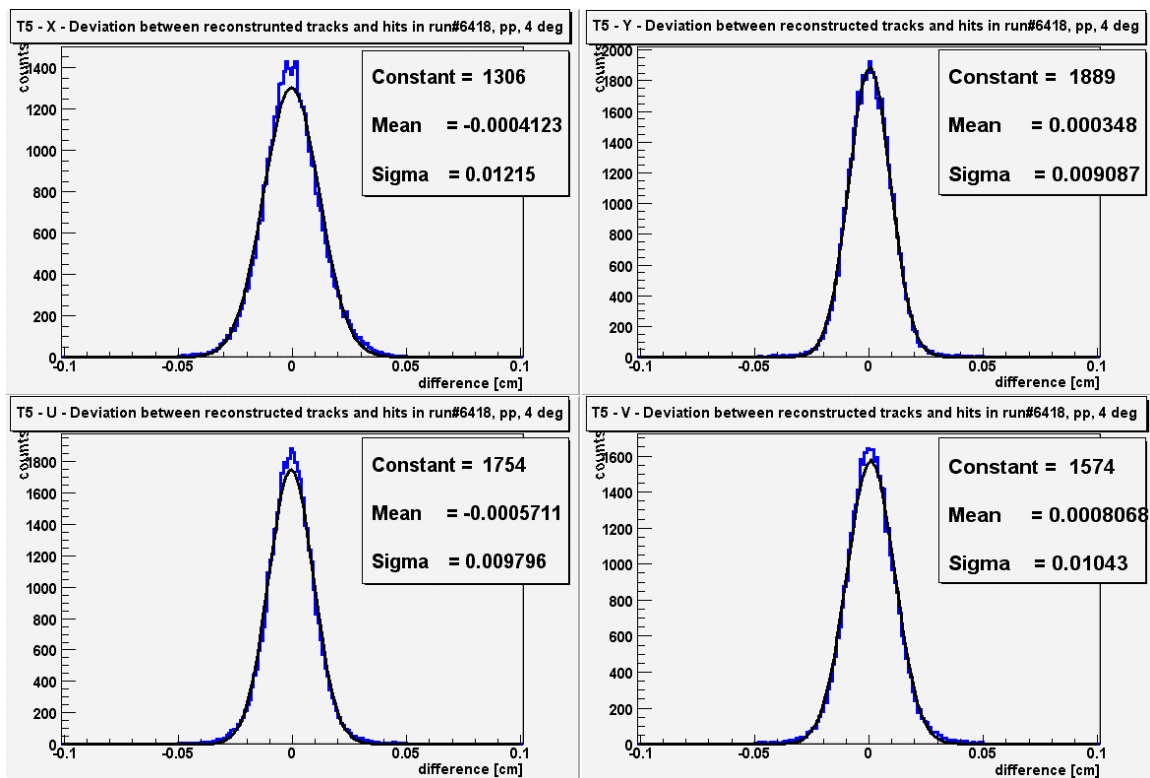


Fig.19. Resolution of the reconstructed tracks in the T5 detector.

## 4. Efficiency

### 4.1 Justification of the efficiency optimization

One of the most important things in the experimental physics and in the case of the detectors is the matter of efficiency. It is generally known that each wire can be ineffective due to various reasons. The tracking method may also be ineffective. Already presented improved tracking method increases the efficiency in two of the BRAHMS detectors, that is in the T3 and T5. Assuming that the efficiency of the drift chamber is equal to 90% and that after applying the new tracking method the efficiency increases to 95% it is easy to observe that the

overall BFS efficiency increases from  $90\% \cdot 90\% \cdot 90\% = 72.9\%$  to  $95\% \cdot 90\% \cdot 95\% = 81.225\%$ , which is a 10% increase. Assuming possible extensions to another detectors the global efficiency increases greatly.

#### 4.2 Methods of calculating the efficiency

The efficiency of the drift chamber is defined as the ratio of the reconstructed (using standard (local) or new (see sec. 3.2.3) tracking method). Confirmation of the track by the time-of-flight wall may additionally serve for the efficiency calculation of the TOF detector. In the tracking module I have devised two ways of calculating the efficiencies of different detectors.

The first method is strictly connected with the tracking process. Figure 20 depicts the matched track (MT) numbers that will be used to calculate the efficiencies.

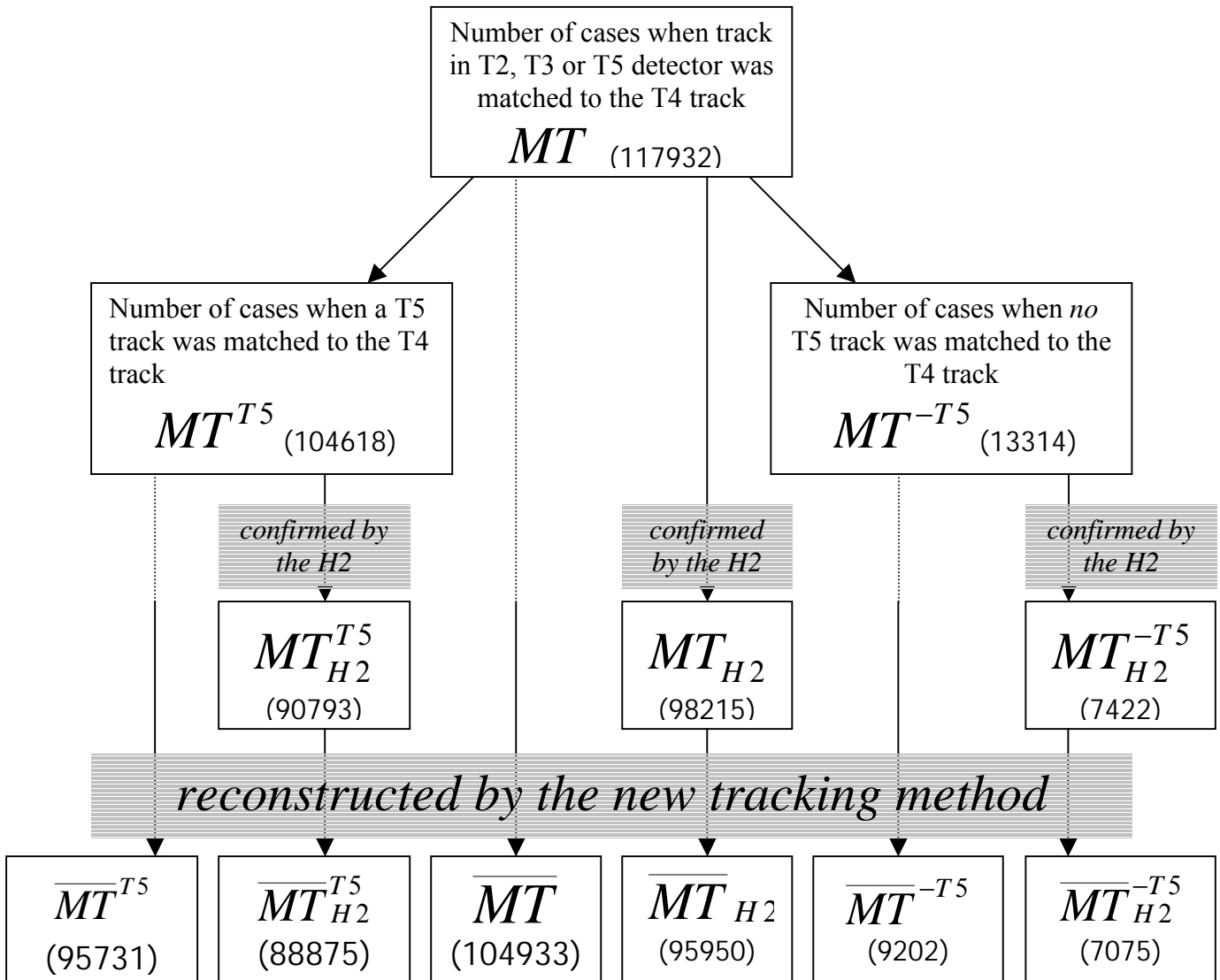


Fig. 20. Description of the numbers used to calculate the efficiencies. The values are obtained from the run #6418 (proton run with BFS at 4°).

In order to calculate different types of efficiencies it is necessary to take the ratios of two numbers from diagram in Fig. 20 that have one indice different *only*:

- The efficiency of H2 can be calculated as the ratio of the number with ‘H2’ and similar without ‘H2’, e.g.

$$Eff(H2) = MT_{H2}^{T5} / MT_{H2}^{T5 \#6418} = 90793 / 104618 = 86.79\%,$$

- The efficiency of the standard tracking method in the T5 is equal to the ratio of the number with ‘T5’ and similar without ‘T5’, e.g.

$$Eff(s.t.m.) = MT_{H2}^{T5} / MT_{H2}^{T5 \#6418} = 90793 / 98215 = 92.44\%,$$

- The efficiency of the new tracking procedure (which is not the efficiency of the detector) is the ratio of the number with with the bar to similar one without bar, e.g.

$$Eff(n.t.m.) = \overline{MT}_{H2}^{T5} / MT_{H2}^{T5 \#6418} = 88875 / 90793 = 97.89\%.$$

Efficiencies calculated in this way are presented in the Tables 5 and 6. Figure 21 presents the efficiencies of the tracking methods in the T5 detector versus the  $x$  position (at  $z=0$ ) of the projected track.

Table 5. Efficiencies of the tracking methods for the the T5 detector in run #6418.

<b>T5</b> run #6418	standard $MT^{T5} / MT$	new tracking method		
		$\overline{MT}^{-T5} / MT^{-T5}$	$\overline{MT}^{T5} / MT^{T5}$	$\overline{MT} / MT$
all	88.71%	69.12%	91.51%	88.98%
H2 confirmed	92.44%	95.32%	97.89%	97.69%

Table 6. Efficiencies in the H2.

<b>H2</b> run #6418	all projected tracks $MT_{H2} / MT$	reconstructed tracks $\overline{MT}_{H2} / \overline{MT}$
all	83.28%	91.44%
T5 confirmed	86.79%	92.84%

The new tracking method was designed to be applied to the cases when no track in the T5 detector was found using standard (local) method. It means that the efficiency of the T5 detector can be calculated as the ratio of the number of the cases when track in the T5 was found using either standard or new tracking method ( $MT^{T5} \oplus \overline{MT} = MT^{T5} + \overline{MT}^{-T5}$ ) to the number of all matched tracks ( $MT$ ). If additionally the track is confirmed by H2 new efficiency of the T5 detector is obtained:

$$Eff(T5) = (MT_{H2}^{T5} \oplus \overline{MT}_{H2}) / MT_{H2} = (MT_{H2}^{T5} + \overline{MT}_{H2}^{-T5}) / MT_{H2} \#6418 = (90793 + 7075) / 98215 = 99.65\%$$

Table 7 presents the efficiencies for different detectors before and after applying new tracking methods, for the run #6418.



Table 7. Efficiencies of various detectors before and after improvement – method 1.

#6418	<b>T3</b>		<b>H1</b>		<b>T5</b>		<b>H2</b>	
	all	H1 conf.	All	T3 conf.	All	H2 conf.	All	T5 conf.
before	98.45%	99.51%	—	—	88.71%	92.44%	—	—
after	98.76%	99.81%	98.10%	99.70%	96.51%	99.65%	83.28%	91.44%

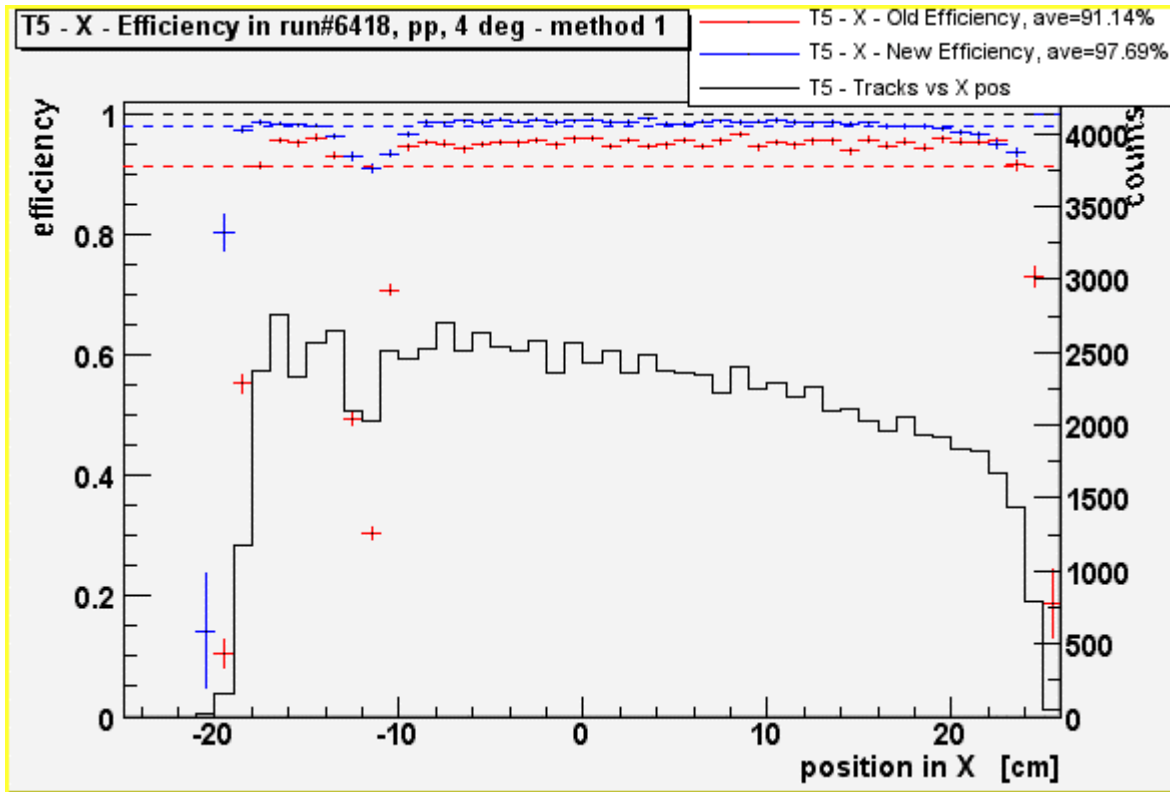


Fig. 21. Efficiency in the T5 - method 1.

The second method of calculating the efficiency is based on the fact that the reconstruction of the track in even three detectors (e.g. T2, T3 and T4) does not mean that it belonged to a particle that travelled from the interaction region all way down to the RICH detector. It is because in the single event a great number of particles is created. These particles travel all over the experimental hall and can scatter or produce secondary particles on the magnets, detectors and other things which happen to be in the hall as well as in the medium itself (the air or gas). It is therefore reasonable to look for the events where all (T2, T3, T4, T5 and H1, H2) detectors detected the particle and compare them with the events where one detector confirmation is missing. The efficiencies using this method are summarized in the Tables 8 and 10 and Fig. 22.

Table 8. Efficiencies of various detectors before and after T3 improvement – method 2.

#6418	H1	T3	T5	H2
before	99.56%	99.89%	95.40%	95.14%
after	99.56%	99.96%	95.39%	95.14%

Table 9. Efficiencies of various detectors before and after improvement – method 2.

#6418	H1	T3	T5	H2
before	99.54%	99.89%	95.46%	95.12%
after	99.55%	99.88%	99.21%	95.05%

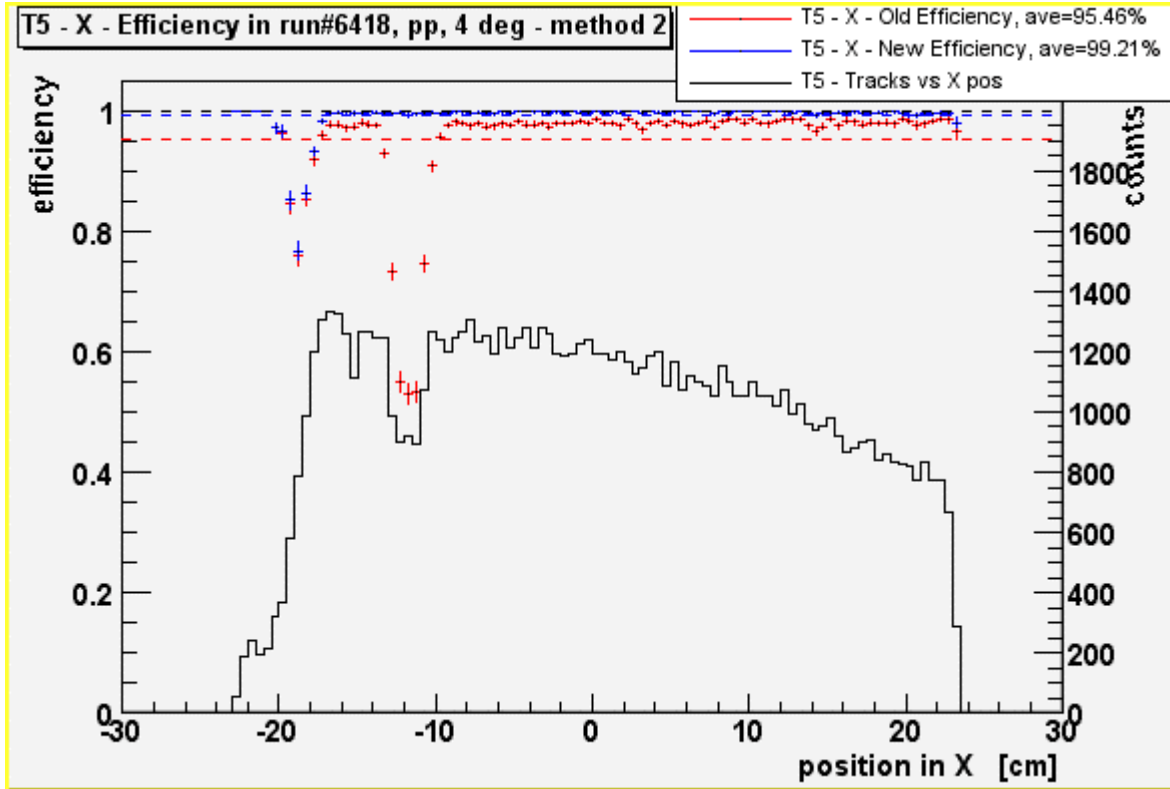


Fig. 22. Efficiency in the T5 – method 2.

## 5. Results

### 5.1 Track resolution in the drift chambers

The track resolution for tracks reconstructed using the software presented in sec. 3.2.3 is presented in the Table 10.

Table 10. Track resolution in various views in T3 and T5 detectors .

resolution in the T3						resolution in the T5			
X views	Y views	U views	V views			X views	Y views	U views	V views
[ $\mu\text{m}$ ]	[ $\mu\text{m}$ ]	[ $\mu\text{m}$ ]	[ $\mu\text{m}$ ]	Run#	info	[ $\mu\text{m}$ ]	[ $\mu\text{m}$ ]	[ $\mu\text{m}$ ]	[ $\mu\text{m}$ ]
142.2	119.3	123.1	128.4	5677	12AuAu	136.8	116.1	118.1	127.2
143.5	116.4	129	131.2	5680	12AuAu	130.6	106.9	111.4	112.1
140.5	115.6	126.8	125.7	5692	12AuAu	127.2	103.5	109.6	111.1
140	116	120.2	130.6	5696	12AuAu	124.9	110.2	112.7	116.1
172.1	160.1	178.2	180.2	5931	4AuAu	116.2	90.74	98.07	117.5
141	108.1	113.7	120.1	6192	8pp	127	99.71	108.5	101.8
127.4	134	114.8	120.5	6211	8pp	110.5	84.84	94.34	95.13
131.2	104.7	103.3	108.5	6215	8pp	115.6	89.3	101.5	99.44
122.2	88.41	90.27	96.57	6415	4pp	110.7	90.42	89.14	94.27
132	94.79	107.1	106.6	6418	4pp	121.5	90.87	97.96	104.3
128.4	91.03	97.97	101.6	6488	3pp	112	87.72	92.87	97.96

### 5.2 Efficiency of the drift chambers

The efficiencies calculated using the second method described in sec. 4.2 before and after applying the software presented in sec. 3.2.3 are presented in the Tables 11 and 12 for T5 and T3 improvement, respectively.

Table 11. Efficiencies in various detectors before and after applying the new tracking method to the T5 detector.

		T5 improvement							
		H1		T3		T5		H2	
Run#	run info	before	after	before	after	before	after	before	after
5677	12AuAu	98.80%	98.81%	97.72%	97.58%	93.69%	98.89%	96.72%	96.62%
5680	12AuAu	98.70%	98.68%	98.23%	98.13%	94.51%	98.88%	96.63%	96.64%
5692	12AuAu	98.51%	98.51%	98.11%	97.86%	93.34%	98.81%	96.76%	96.79%
5696	12AuAu	98.93%	98.89%	98.40%	98.31%	95.48%	99.35%	95.90%	95.83%
5931	4AuAu	98.17%	98.23%	85.47%	83.31%	91.16%	98.34%	97.91%	97.81%
6192	8pp	99.36%	99.39%	99.75%	99.75%	96.49%	99.35%	95.41%	95.35%
6211	8pp	98.69%	98.49%	99.92%	99.95%	96.98%	99.40%	96.75%	96.76%
6215	8pp	99.51%	99.51%	99.92%	99.91%	96.82%	99.47%	95.16%	95.12%
6415	4pp	99.27%	99.29%	99.93%	99.91%	94.83%	98.81%	96.38%	96.29%
6418	4pp	99.54%	99.55%	99.89%	99.88%	95.46%	99.21%	95.12%	95.05%
6488	3pp	99.42%	99.42%	99.88%	99.88%	95.44%	99.21%	95.61%	95.51%

Table 12. Efficiencies in various detectors before and after applying the new tracking method to the T3 detector.

		T3 improvement							
		H1		T3		T5		H2	
Run#	run info	before	after	before	after	before	after	before	After
5677	12 <sub>AuAu</sub>	98.71%	98.20%	97.71%	99.55%	93.59%	93.57%	96.71%	96.62%
5680	12 <sub>AuAu</sub>	98.70%	98.70%	98.24%	99.60%	94.30%	99.18%	96.65%	96.67%
5692	12 <sub>AuAu</sub>	98.53%	98.53%	98.13%	99.61%	93.20%	92.97%	96.82%	96.83%
5696	12 <sub>AuAu</sub>	99.02%	99.04%	98.39%	99.79%	95.38%	95.33%	96.08%	96.01%
5931	4 <sub>AuAu</sub>	98.13%	98.24%	85.80%	94.79%	90.60%	88.88%	97.90%	97.79%
6192	8 <sub>pp</sub>	99.36%	99.36%	99.25%	99.91%	96.43%	96.42%	95.42%	95.41%
6211	8 <sub>pp</sub>	99.88%	99.69%	99.92%	100.00%	96.75%	96.75%	96.83%	96.75%
6215	8 <sub>pp</sub>	99.51%	99.51%	99.92%	99.96%	96.80%	96.79%	95.14%	95.15%
6415	4 <sub>pp</sub>	99.28%	99.28%	99.93%	100.00%	94.86%	94.82%	96.75%	96.36%
6418	4 <sub>pp</sub>	99.56%	99.56%	99.89%	99.96%	95.40%	95.39%	95.14%	95.13%
6488	3 <sub>pp</sub>	99.44%	99.44%	99.88%	99.99%	95.42%	95.42%	95.63%	95.62%

## 6. Conclusions

### 6.1 Usefulness of the introduced software in the BRAHMS

The BRAHMS experiment software – BRAT – is still in its development stage. The main task now is to finish the tracking procedure so that fast particle and momentum identification were possible. The software presented here (i.e. BrDcRdoModule) greatly simplifies the usage of the drift chambers' software by means of eliminating the necessity of using the calibration and geometrical classes (BrDcCalibration and BrDriverDC) which, if used in an improper way, could easily lead to mistakes. The second of the described programs – BrDcEnhancement – improves the efficiency of the drift chambers in the BRAHMS experiment. The increase in the efficiency in both T3 and T5 detectors does not cause problems in the neighboring detectors and the track resolution is very high. Actually the achieved track resolution is close to 100 $\mu$ m (see Table 9), and in the worse case of T3 detector with the FS at 4° for the gold-gold run it drops to 180 $\mu$ m, which is still much better than the designed resolution, which was 300 $\mu$ m – see 1.2.2, [3].

### 6.2 Possible extensions to the whole FS – farther development

The software presented here, namely the new method of tracking, can be extended to other detectors. For example the T1 detector is not performing too well and the tracking procedure similar to that applied in the BrDcEnhancement could greatly improve its performance. The detectors used in this case would be T2, T3 and T4 and the momentum would be taken from T2-T4 and T3-T4 matched tracks.

The other possible development could be to use the time-of-flight hits, which now serve only as a track confirmation, to create matched tracks (e.g. T4-H2 tracks) and then to confirm them (using the method analogical to that described in sec. 3.2.3) in the T5 detector. The main problems in this case would be the difficulty in obtaining the momentum (because only the track entering the magnet is available) and the number of possible connections, in the case of several hits on the TOF wall. However these problems could probably be solved and yet higher level in the efficiencies would be achieved.

The farther developments of the tracking software in the BRAHMS analysis is a crucial task for the optimalization of the data processing.

#### References:

1. I.G. Bearden *et al.* (BRAHMS), Phys. Lett. **B523** (2001) 227-233, nucl-ex/0108016.
2. I.G. Bearden *et al.* (BRAHMS), Phys. Rev. Lett. 88 (2002), nucl-ex/0112001.
3. D. Beavis *et al.* (BRAHMS), 'Conceptual Design Report for the BRAHMS experiment', ([/www4.rcf.bnl.gov/brahms/WWW/cdr/cdr.html](http://www4.rcf.bnl.gov/brahms/WWW/cdr/cdr.html)).
4. Z. Majka *et al.*, 'Drift chambers for the BRAHMS experiment at RHIC' (unpublished).
5. Christian Holm, 'The Hitchhikers Guide to BRAT – DON'T PANIC' ([/pii3.brahms.bnl.gov/~brahmlib/brat/guide/](http://pii3.brahms.bnl.gov/~brahmlib/brat/guide/)).
6. The ROOT System Home Page ([/root.cern.ch/](http://root.cern.ch/)).

## Appendix A

### The BRAHMS Collaboration

G. Bearden<sup>7</sup>, D. Beavis<sup>1</sup>, C. Besliu<sup>10</sup>, Y. Blyakhman<sup>6</sup>, B. Budick<sup>6</sup>,  
H. Bøggild<sup>7</sup>, C. Chasman<sup>1</sup>, C. H. Christensen<sup>7</sup>, P. Christiansen<sup>7</sup>,  
J. Cibor<sup>3</sup>, R. Debbe<sup>1</sup>, E. Enger<sup>12</sup>, J. J. Gaardhøje<sup>7</sup>, M. Germinario<sup>7</sup>,  
K. Hagel<sup>8</sup>, O. Hansen<sup>7</sup>, A. Holm<sup>7</sup>, A. K. Holme<sup>12</sup>, H. Ito<sup>1</sup>,  
E. Jakobsen<sup>7</sup>, A. Jipa<sup>10</sup>, F. Jundt<sup>2</sup>, J. I. Jørdre<sup>9</sup>, C. E. Jørgensen<sup>7</sup>,  
R. Karabowicz<sup>4</sup>, T. Keutgen<sup>8</sup>, E. J. Kim<sup>1</sup>, T. Kozik<sup>4</sup>,  
AA. T. M. Larsen<sup>12</sup>, J. H. Lee<sup>1</sup>, Y. K. Lee<sup>5</sup>, G. Løvhøiden<sup>12</sup>, Z. Majka<sup>4</sup>,  
A. Makeev<sup>8</sup>, B. McBreen<sup>1</sup>, M. Mikelsen<sup>12</sup>, M. Murray<sup>8</sup>,  
J. Natowitz<sup>8</sup>, B. S. Nielsen<sup>7</sup>, J. Norris<sup>11</sup>, K. Olchanski<sup>1</sup>,  
J. Olness<sup>1</sup>, D. Ouerdane<sup>7</sup>, R. Płaneta<sup>4</sup>, F. Rami<sup>2</sup>,  
D. Röhrich<sup>9</sup>, B. H. Samset<sup>12</sup>, D. Sandberg<sup>7</sup>, S. J. Sanders<sup>11</sup>,  
R. A. Sheetz<sup>1</sup>, P. Staszal<sup>7</sup>, T. F. Thorsteinsen<sup>9†</sup>, T. S. Tveter<sup>12</sup>,  
F. Videbæk<sup>1</sup>, R. Wada<sup>8</sup>, A. Wieloch<sup>4</sup>, I. S. Zgura<sup>10</sup>

1. Brookhaven National Laboratory, Upton, New York 11973, USA
2. Institut de Recherches Subatomiques and Université Louis Pasteur, Strasbourg, France
3. H. Niewodniczanski Institute of Nuclear Physics, Kraków, Poland
4. M. Smoluchowski Institute of Physics, Jagiellonian University, Kraków, Poland
5. John Hopkins University, Baltimore, Maryland 21218, USA
6. New York University, New York, New York 10003, USA
7. Niels Bohr Institute, University of Copenhagen, Denmark
8. Cyclotron Institute, Texas A&M University, College Station, Texas 77843, USA
9. University of Bergen, Department of Physics, Bergen, Norway
10. University of Bucharest, Romania
11. University of Kansas, Lawrence, Kansas 66045, USA
12. University of Oslo, Department of Physics, Oslo, Norway

† Deceased

## Appendix B

The BRAT Classes (selected):

### Data classes:

BrDataTable – a collection of any type of data, organized in objects belonging to the classes deriving from the BrDataObject.

BrDcDig – drift chambers digitized data, containing specific number of data, which can be described as:

- id of the hit,
- the number of the module (1,2 or 3),
- the number of the plane (for range – refer to Table 1),
- the number of the wire (for range – refer to Table 1),
- the TDC signal (see sec. 1.2.2),
- the width of the signal (only in the case of the T3).

BrDetectorHit – class used for storing hits, is not dedicated to any specific detector.

BrDetectorTrack – class for containing local tracks, is not limited to the drift chambers, can contain tracks from any detector. It incorporates, among others, the following data:

- id of the track,
- the position of the track in the  $xy$  plane (in the form of BrVector3D: {position in  $x$ , position in  $y$ , 0}),
- the slope of the track, also as BrVector3D: { $x$  slope,  $y$  slope, 1},
- the status, or the quality, of the track.

BrMatchedTrack – first step towards global tracking, contains pointers to the tracks in two detectors separated by a magnet, the momentum of the particle reconstructed from the tracks entering and exiting the magnet, and the status, which describes the quality of the connection.

BrBfsTrack – container for two BrMatchedTrack, generally combines tracks locally found in the drift chambers into one object, constructed analogically to the BrMatchedTrack.

BrFsTrack – the class for containing the global tracks, constructed similarly to the BrMatchedTrack and BrBfsTrack. It contains all the reconstructed information about the particle: its kind, charge, momentum, mass, time-of-flight and so on.

### Modules:

BrDcRdoModule (see sec. 2.2.1) – basing on the raw data, geometry and calibration files creates the BrDataTable of reduced data objects, in the form of BrDetectorHits, that contain the following numbers:

- the position of the hit which is equal to: position of the wire  $\pm$  drift distance (actually two numbers),
- the position of the plane (in z direction),
- the number of the wire,
- combination of the number of the module (M) and of the plane (P), in the form of  $100 \cdot M + P$ .

BrDCClusterFinder – the module that combines hits in the drift chambers into clusters.

BrDCTrackingModule – the module that combines clusters in the drift chambers into tracks.

BrModuleMatchTrack – the module that creates BrMatchedTracks from the local tracks.

BrBfsTrackingModule – the module that constructs BrBfsTrack from two BrMatchedTracks found for the drift chambers.

BrDcEnhancement – the module that improves the drift chambers' efficiencies using other detectors (see sec. 3.2.3).

Managers:

BrCalibrationManager – the manager class that is responsible for applying the same calibration (there are many versions as the software is still being developed) in the data processing.

BrGeometryDbManager – responsible for geometry (see BrCalibrationManager).

BrParameterDbManager – responsible for the parametrization (see BrCalibrationManager).

Utilities:

BrDriverDC – geometry and other hardware information (e.g. the number of the modules, wires) for the drift chambers.

BrDcCalibration – calibration of the drift chambers.